ACS Medicinal Chemistry Letters

Letter

Cite This: ACS Med. Chem. Lett. 2018, 9, 198−203

Unraveling the Binding, Proton Blockage, and Inhibition of Influenza M2 WT and S31N by Rimantadine Variants

Antonios Drakopoulos,[†] Christina Tzitzoglaki,[†] Kelly McGuire,[‡] Anja Hoffmann,[§] Athina Konstantinidi,[†] Dimitrios Kolokouris,[†] Chunlong Ma,[∥] Kathrin Freudenberger,[⊥] Johanna Hutterer,[⊥] Günter Gauglitz,[⊥] Jun Wang,[∥] Michaela Schmidtke,[§] David D. Busath,[‡] and Antonios Kolocouris*[,†]

[†]Department of Pharmaceutical Chemistry, Faculty of Pharmacy, National and Kapodistrian University of Athens, Panepistimiopolis-Zografou 15771, Greece

[‡]Department of Physiology and Developmental Biology, Brigham Young University, Provo, Utah 84602, United States

[§]Department of Medicinal Microbiology, Section Experimental Virology, Jena University Hospital, Hans Knoell Str. 2, D-07745 Jena, Germany

[∥]Department of Pharmacology and Toxicology, College of Pharmacy, University of Arizona, Tucson, Arizona 85721, United States

[⊥]Institut für Physikalische und Theoretische Chemie, Eberhard-Karls-Universität Tübingen, 72074 Tübingen, Germany

Supporting Information

ABSTRACT: Recently, the binding kinetics of a ligand−target interaction, such as the residence time of a small molecule on its protein target, are seen as increasingly important for drug efficacy. Here, we investigate these concepts to explain binding and proton blockage of rimantadine variants bearing progressively larger alkyl groups to influenza A virus M2 wild type (WT) and M2 S31N protein proton channel. We showed that resistance of M2 S31N to rimantadine analogues compared to M2 WT resulted from their higher k_{off} rates compared to the k_{on} rates according to electrophysiology (EP) measurements. This is due to the fact that, in M2 S31N, the loss of the V27 pocket for the adamantyl cage resulted in low residence time inside the M2 pore. Both rimantadine enantiomers have similar channel blockage and binding k_{on} and k_{off} against M2 WT. To compare the potency between the rimantadine variants against M2, we applied approaches using different mimicry of M2, i.e., isothermal titration calorimetry and molecular dynamics simulation, EP, and antiviral assays. It was also shown that a small change in an amino acid at site 28 of M2 WT, which does not line the pore, seriously affects M2 WT blockage kinetics.

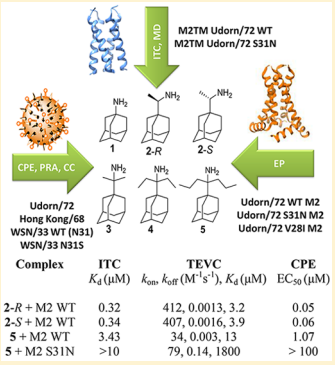

Complex	ITC K_d (μM)	TEVC k_{on}, k_{off} ($M^{-1}s^{-1}$), K_d (μM)	CPE EC_{50} (μM)
2-*R* + M2 WT	0.32	412, 0.0013, 3.2	0.05
2-*S* + M2 WT	0.34	407, 0.0016, 3.9	0.06
5 + M2 WT	3.43	34, 0.003, 13	1.07
5 + M2 S31N	>10	79, 0.14, 1800	> 100

KEYWORDS: *Influenza M2, S31N mutation, rimantadine, rimantadine enantiomers, isothermal titration calorimetry, electrophysiology, binding kinetics, synthesis, antiviral assay, molecular dynamic simulations*

Novel approaches are necessary in early drug discovery for optimal drug design and improved therapy. Recently, the kinetics of a ligand−target interaction, such as the residence time of a small molecule on its protein target, are seen as increasingly important for *in vivo* efficacy and safety.[1]

The antiviral agents amantadine (**1**) and rimantadine (**2**) (Scheme 1) are well-established to be blockers of proton transport by the influenza A virus (IAV).[2,3] The primary binding site of **1** and **2** is the transmembrane domain lumen (TM, amino acids 22−46) in the four-helix bundle of tetrameric M2, which forms the proton transport path.[2] Since 2008, high-resolution structures have become available for complexes of M2TM wild type (WT) with **1** or **2** (Figure S1).[4−9]

Scheme 1. Structures of Aminoadamantane Derivatives 1−5

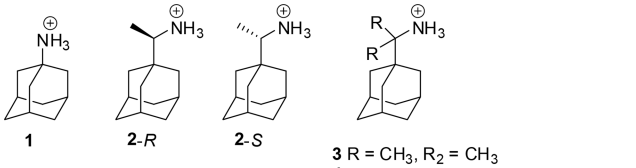

1 **2**-*R* **2**-*S*

3 R = CH_3, R_2 = CH_3
4 R = CH_2CH_3, R_2 = CH_2CH_3,
5 R = $CH_2CH_2CH_3$, R_2 = $CH_2CH_2CH_3$

Compounds **1** and **2** are effective prophylactics and therapeutics against IAVs, provided they contain the M2TM WT such as A/Udorn/72 H3N2 (Udorn) and A/Hong Kong/68 H3N2 (HK), but not those containing M2 S31N such as A/WSN/33 H1N1 (WSN) (Figure S2). Since 2005, the amantadine (1)-insensitive Ser-to-Asn mutation at position 31 in M2 (S31N) has become globally prevalent, abrogating the clinical usefulness of **1**.[10]

Compound **2** is ranked among the best binders to M2TM WT[11,12] and most potent anti-IAV agents among the amino-adamantane derivatives.[13,14] Thus, the synthesis of symmetrical

Received: November 3, 2017
Accepted: January 29, 2018
Published: January 29, 2018

DOI: 10.1021/acsmedchemlett.7b00458
ACS Med. Chem. Lett. 2018, 9, 198−203

analogues of **2** with the addition of two methyl (**3**), ethyl (**4**), and n-propyl (**5**) groups on the carbon bridge was accomplished (Scheme 1) aiming at filling progressively from **3** to **5** the extra space between the ligand and the walls in M2 WT or M2 S31N with a few alkyl groups. Binding affinities of **1**, **2**, **2**-*R*, **2**-*S*, and **3**−**5** were measured by ITC against the M2TM WT and its S31N variant in their closed form at pH 8. Furthermore, we measured the antiviral activity of the rimantadine analogues against IAV strains and the blocking effect of the compounds against full length Udorn M2, Udorn M2 S31N, and Udorn M2 V28I using electrophysiology (EP), and the kinetics of binding were compared. Molecular dynamics (MD) simulations of ligand binding to M2TM WT and its S31N variant in their closed form were performed for investigation of the binding mode interactions.

For the synthesis of primary *tert*-alkyl amines **3**−**5**, the raw *tert*-alkyl alcohols **7a**−**c** were prepared according to Scheme 2 from

Scheme 2. Synthetic Scheme for the Preparation of Compounds 3−5

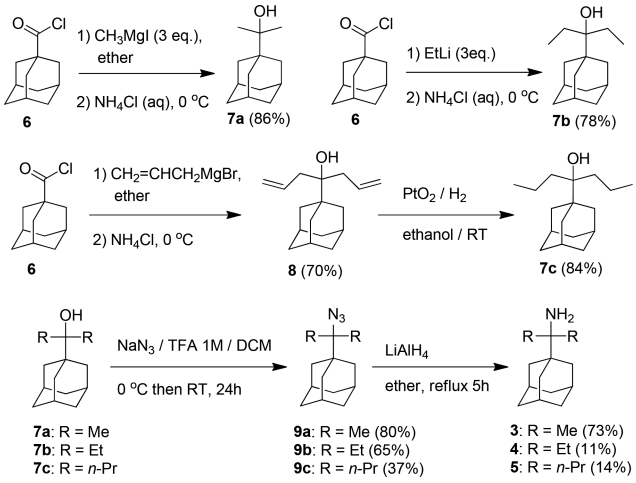

the reaction between 1-adamantanecarbonyl chloride **6** and an organometallic reagent (see Supporting Information). It was reported that the reaction of 1-adamantanecarbonitrile with ethyl magnesium bromide and titanium tetraisopropoxide afforded **4** in 52% yield.[15] We tested twice this procedure with 1-adamantanecarbonitrile and methylmagnesium bromide yielding in our hands **3** with only 10% yield, which is lower than the ∼50% yield starting from **6** or 1-adamantanecarboxylic acid (Scheme 2).

Table 1 includes thermodynamic parameters of binding against M2TM WT and M2TM S31N. Binding affinities were determined by ITC for M2TM−ligand systems in dodecylphosphocholine (DPC) micelles at pH 8, where M2TM fragments form stable tetramers (see also Supporting Information).[16] Compound **1** has a K_d of 2.17 μM. As depicted in Table 1, enantiomers **2**-*R* and **2**-*S* have the same K_d values[17] against M2TM WT (K_d = 0.34 and 0.32 μM, respectively). Compound **3**, having two methyl groups instead of one methyl group in **2**, has the smallest K_d = 0.13 μM, i.e., the highest binding affinity of all studied aminoadamantane compounds, suggesting that polar and lipophilic characteristics are well balanced in its structure. The diethyl derivative **4** and dipropyl derivative **5** exhibit lower binding affinities against M2TM WT (K_d = 4.59 and 3.43 μM, respectively). A balance between enthalpy and entropy determines the free energy of binding as shown in Table 1. The entropy presumably changes significantly from **1**, **2** to **3**, **4** on binding because the ordered clathrate water surrounding the ligand is dispersed as the ligand enters the water-poor channel cavity. This is more prominent for **3** and **4**, as expected due to their larger hydrophobic surfaces. Presumably, it would have gone up even more for **5**, but this clathrate effect was probably countered by a reduced ligand entropy in the channel due to restricted rotation inside the receptor binding area. Compounds **1**−**3** did not bind efficiently to M2TM S31N according to isothermal titration calorimetry (ITC) and previous surface plasmon resonance measurements for **1**,[18] while **5**, with a larger adduct connected to adamantane, binds weakly to M2TM S31N compared to M2TM WT according to ITC.

The cytopathic effect (CPE) inhibition assay was used[19] to compare the antiviral potency of **1**−**5** against HK, Udorn, WSN, and WSN M2 N31S (generated by reverse genetics from WSN) in MDCK cells (Table 2). The amino acid sequences of M2 WT in Udorn and HK are identical, not just in the TM region but in the full length protein. There was no potency against the amantadine-resistant WSN with the compound concentrations used. All compounds showed low micromolar activity against Udorn, HK, and WSN M2 N31S with **3** being the most potent agent exhibiting submicromolar potency. Inhibition of repli-

Table 1. Binding Constant, Free Energy, Enthalpy, and Entropy of Binding at 300 K Derived from ITC Measurements for M2TM WT (from Udorn, Upper Table) and the M2TM S31N (Lower Table)

ligand[a]	K_d[b]	ΔG[c]	ΔH[d]	$-T\Delta S$[e]
		M2TM WT		
1	2.17 ± 0.52	−7.77 ± 0.14	−6.66 ± 0.50	−1.11 ± 0.52
2	0.51 ± 0.26	−8.64 ± 0.30	−7.60 ± 0.28	−1.04 ± 0.41
2-*R*	0.32 ± 0.16	−8.97 ± 0.26	−7.54 ± 0.34	−1.42 ± 0.43
2-*S*	0.34 ± 0.12	−8.88 ± 0.21	−7.73 ± 0.28	−1.15 ± 0.35
3	0.13 ± 0.12	−9.30 ± 0.43	−4.19 ± 0.28	−5.12 ± 0.51
4	4.59 ± 2.21	−7.33 ± 0.28	−3.29 ± 0.62	−4.03 ± 0.68
5	3.43 ± 1.05	−7.50 ± 0.18	−6.23 ± 0.45	−1.27 ± 0.48
		M2TM S31N		
1−**3**	*f*	*f*	*f*	*f*
5	>10	*f*	*f*	*f*

[a]See Scheme 1. [b]Binding constant K_d in μM [2]. [c]Free energy of binding in kcal mol^{-1}. [d]Binding enthalpy in kcal mol^{-1}. [e]Entropy of binding in kcal mol^{-1}. [f]Values could not be determined reliably due to the limitations of the methods in the area of very weak binding (see also SI for definition of quantities).

DOI: 10.1021/acsmedchemlett.7b00458
ACS Med. Chem. Lett. 2018, 9, 198−203

Table 2. Cytotoxicity (CC_{50}) and Antiviral Activity (EC_{50}) of Compounds 1−5 against IAVs HK, Udorn, WSN, and WSN M2 N31S in Madin−Darby Canine Kidney Cells

	EC_{50} (μM)[a]				
	HK	Udorn	WSN		
ligand	M2 (V28; S31)	M2 (V28; S31)	M2 (I28; N31S)	M2 (I28; N31)	CC_{50} (μM)[a]
1	ND[c]	0.78 ± 0.44	0.48 ± 0.05	>100	>100
2	0.05 ± 0.04	0.09 ± 0.03	0.04 ± 0.02	>100	>100
2-*R*	ND[c]	0.05 ± 0.01	0.04 ± 0.01	>100	>100
2-*S*	ND[c]	0.06 ± 0.02	0.02 ± 0.01	>100	>100
3	0.012 ± 0.003	0.01 ± 0.001	0.03 ± 0.02	>100	>100
4	0.46 ± 0.25	0.41 ± 0.23	1.01 ± 0.13	>100	>100
5	0.45 ± 0.34	1.07 ± 0.31[b]	1.06 ± 0.23	>100	57.3 ± 11.3
Oseltamivir	0.002 ± 0.001	0.001	0.02 ± 0.01	0.03 ± 0.01	>100

[a]Mean and standard deviations of the 50% inhibitory concentration (EC_{50}) and the 50% cytotoxic concentration (CC_{50}) of at least three independent assays. [b]Inhibition of plaque size without reduction of plaque number. [c]ND: Not determined.

cation of Udorn was further confirmed with plaque-reduction assay (results not shown). It is of note that **5** only reduced the plaque size but not the number of plaques. The cytotoxicity data (Table 2) showed that **1**−**4** are nontoxic with CC_{50} values >100 μM, but **5** is mildly toxic with $CC_{50} \approx 57$ μM.

The EC_{50} values for **1**−**5** (Table 2) prioritize the same derivative for M2 WT virus inhibition, i.e., **3**, in agreement with the results from the K_d values from ITC experiments based on M2TM WT binding (Table 1). Compound **3** is almost equal in structure with rimantadine (**2**) without having a chiral center. Compound **3** has also a promising selectivity index based on the *in vitro* cytotoxicity data.

The inhibitors were tested with a two-electrode voltage clamp (TEVC) assay using *X. laevis* frog oocytes microinjected with RNA expressing the M2 protein as in previous reports.[13,17] The blocking effect of the aminoadamantane derivatives against M2 was investigated with EP experiments using Udorn M2 and Udorn M2 S31N. Because WSN has the V28I substitution in M2, Udorn M2 V28I was generated and studied in parallel to examine whether small changes in WSN in the side chains of amino acids that do not line the pore (Figure S2) affect aminoadamantane blocking properties. The blocking effect of the inhibitors was expressed as the inhibition percentage of the M2 current observed after 2, 5, and/or 10 min of incubation with 100 μM compound (Tables 3 and S1).

After 5 min, **3** and **4** block Udorn M2 and Udorn M2 V28I as well as **1** (about 90% and 80%, respectively). Generally, after 2 and 5 min, the percentage of current inhibition was progressively increased for **3** and **4**. It is noteworthy that **5** against Udorn M2 exhibited 27% blocking at 2 min, 38% at 5 min, and 61% at 10 min (Table 3). The IC_{50} values of **3** and **4** for Udorn M2 and Udorn M2 V28I were reduced from 2 to 5 min time points (Tables 3 and S1). These measurements at 2, 5, or 10 min are made prior to the establishment of equilibrium[21] due to very slow on- and off-rates for entry (see the k_{on} and k_{off} rate values in Tables 3 and 4), especially of the bulky ligands like **5**, together with the difficulty of maintaining cells at low pH for extended periods. Thus, the very slow binding of **5** (Table 3) should not be viewed as inconsistent with the high antiviral potency (submicromolar EC_{50}) against WT (V28; S31) viruses (Table 2), the latter representing much longer exposure times than EP experiments.

In a very recent paper,[20] the authors showed that when K_d(TEVC) = k_{off}/k_{on} was smaller than a threshold, an *in vitro* antiviral activity was exhibited. For amantadine (**1**), k_{off}/k_{on} = 10^{-6} M (1 μM) was measured against M2 WT, which correlates with good *in vitro* antiviral potency. When k_{off}/k_{on} ~100 μM or higher, antiviral potency was not observed even for quick binders. For example, 4-(2-adamantyl)piperidine (compound **3** in ref 20), although a quick blocker against Udorn M2 and the amantadine resistant Udorn M2 V27A, was ineffective against the corresponding influenza A strains. The authors also showed that 2-(1-adamantyl)piperidine (compound **8** in ref 20) was a slow binder against Udorn M2 (48% at 2 min, but 90% at 6 min) but still has good antiviral efficacy, possibly because, although k_{on} is low, k_{off} is really low. This is the case with compound **5** against Udorn M2 WT in the present study (see Table 3). It has a reduced onset of block compared to **1**, **2**, and **3**, but also has a low dissociation rate constant, so it still has micromolar efficacy against infections of cell cultures by viral strains with M2 WT.

In studies focusing on the development of aminoadamantane ligands against IAV, derivatives are often initially tested in TEVC assays at 100 μM concentration at 2 min, and only the most potent compounds are then tested using whole cell assays.[21] If the same procedure had been applied here, **5** would not have

Table 3. Block[a] of Inward Currents in Oocytes[b] Transfected with Full-Length Udorn M2 by Selected Compounds

	Udorn M2[a,b]				
ligand	% block (2 min)	% block (5 min)	% block (10 min)	IC_{50} (2 min) (μM)	IC_{50} (5 min) (μM)
1	90 ± 2	95 ± 1	ND[c]	12.5	4.7
2	96 ± 1	96 ± 1	ND[c]	10.8	ND[c]
2-*R*	95 ± 1	96 ± 1	ND[c]	ND[c]	ND[c]
2-*S*	93 ± 1	95 ± 1	ND[c]	ND[c]	ND[c]
3	90 ± 2	96 ± 1	ND[c]	9.3	4.0
4	78 ± 2	91 ± 1	ND[c]	24.3	13.2
5	27 ± 1.2	38 ± 1.6	61 ± 2.3	ND[c]	ND[c]

ligand	k_{on} (M^{-1} s^{-1})	k_{off} (s^{-1})	K_d (μM)[d]
1	327	0.003	9
2	416	0.003	7
2-*R*	412	0.0013	3.2
2-*S*	407	0.0016	3.9
3	230	0.003	13
4	ND[c]	ND[c]	ND[c]
5	34	0.003	88

[a]For each compound, percent block of pH-dependent M2 current at listed concentrations (±SEM) and IC_{50} (μM) are shown. [b]Three replicates were used for measurements at 100 μM. [c]ND: Not determined. [d]K_d (TEVC) = k_{off}/k_{on}.

DOI: 10.1021/acsmedchemlett.7b00458
ACS Med. Chem. Lett. 2018, 9, 198−203

Table 4. Block of Full-Length Udorn M2 S31N-Dependent Current 2 by Selected Compounds[a,b]

	Udorn M2 S31N					
ligand	% block after 2 min	% block after 5 min	% block after 10 min	k_{on} (M^{-1} s^{-1})	k_{off} (s^{-1})	K_d[e]
1	35 ± 2	36 ± 1	36.3 ± 1	143	0.03	210 μM
2[c]	1.0 ± 0.2	1.5 ± 0.4	ND[d]	22	0.9	>10 mM
3	21 ± 2	30 ± 3	33 ± 1	18	0.008	444 μM
5	7.0 ± 0.4	7.6 ± 0.2	8.0 ± 0.4	79	0.14	1.8 mM

[a]For each compound, percent block of pH-dependent M2 current at listed concentrations (±SEM) and IC_{50} (μM) are shown. [b]Three replicates were used for measurements at 100 μM. [c]Racemic. [d]ND: Not determined. [e]$K_d = k_{off}/k_{on}$.

been tested, even though it proved to be a low micromolar inhibitor according to K_d values from ITC experiments with M2TM WT (Table 1) and CPE assay (Table 2) results. Thus, TEVC percent block for 100 μM at 2 min in MDCK cells underestimated the potential of **5**. Similarly **4** would not have been tested based on percent block at 2 min in TEVC with Udorn M2 V28I (Table S1). Slow block could be associated with tight block, and this phenomenon should not be overlooked in short-lasting experiments. The results suggested that TEVC results, when used for compound filtering, need careful interpretation for compounds having low association rate constant for binding to the full length M2, which also depends on the M2 pore. In this regard, ITC measurements represent an important additional tool for clarifying the binding energies of novel derivatives to M2TM given their capacity for sufficient relaxations of equilibrium between titration injections. Nevertheless, it is clear from the ITC, CPE (all strains with M2 WT), that **5** (and **4** where tested) are ∼10-fold less active than **3**.

For Udorn M2 V28I, the percentage of current inhibition is lower; compounds **3** and **4** inhibit Udorn M2 more rapidly than Udorn M2 V28I (Table S1). A small change in an amino acid at site 28 (V28I) of M2, which does not line the pore, seriously affects M2 blockage kinetics. The inhibition of **3** and **4** on both Udorn M2 and Udorn M2 V28I are irreversible in our experimental time frame, as was also observed for **1** with both proteins (data not shown).

After the aforementioned results highlighted the importance of k_{on}, k_{off} values on ligand behavior, we were intrigued to further investigate the block the block of rimantadine enantiomers against Udorn M2 WT protein in EP, considering the differences in resonances seen in ssNMR studies of **2**-*R* or **2**-*S* bound to the full-length Udorn M2 protein.[22] We previously showed[17] that **2**-*R* and **2**-*S* showed similar channel blockage against Udorn M2 WT when tested in EP at 100 μM at the 2- or 5 min time point, and this result is consistent with that from ITC measurements (see ref 17 and Table 1) and antiviral assays (see ref 17 and Table 2). In our present work we seek to further investigate the binding kinetics **2**-*R*, **2**-*S* by measuring the respective k_{on}, k_{off}, K_d (TEVC) values. The EP measurements showed a $k_{off} = 0.0013$ s^{-1} for **2**-*R* and a $k_{off} = 0.0016$ s^{-1} for **2**-*S* (Table 3), i.e., the two enantiomers had very similar binding kinetics. Thus, **2**-*R* has a bit longer residence time inside the receptor than **2**-*S*, as reflected by its slightly lower k_{off} and K_d values (2.4 vs 3.2 μM). In ref 22, the first ssNMR study of the full length M2 in complex with rimantadine enantiomers was published. Compound **2**-*R* was argued to have a higher affinity than **2**-*S* based on differences in peak intensities and position restrained MD simulations. The results published in ref 22 are in qualitative agreement with those reported here, but not in quantitative agreement, as here we see no statistically significant (ITC and EC_{50}) or meaningful (EP) difference. Perhaps this is a consequence of the different methodologies applied, i.e., EP vs ssNMR spectroscopy. Chemical shifts differences and peak intensities do not provide an accurate quantitative estimate of binding affinity values. The EP results, antiviral assays, and ITC results showed clearly that the two rimantadine enantiomers have similar binding free energies, channel blockage, k_{on} and k_{off} rate constants, and antiviral potencies. We conclude that they form equally stable complexes and have the same residence time inside M2 WT.

The compounds did not bind to Udorn M2TM S31N according to ITC and did not exhibit antiviral potency against WSN virus, which contains both the S31N and the V28I mutations. We showed that a valuable parameter to explain the resistance of M2 S31N viruses to rimantadine analogues compared to M2 WT is a higher k_{off} rate (i.e., a smaller residence time inside M2 S31N). According to our previous results, this is due to the fact that, in M2 S31N, the loss of the V27 pocket for the adamantyl cage[11] resulted in low residence time inside M2TM and a lack of antiviral potency; but for **5**, the sizable adducts resulted in a weak binding, which is albeit not sufficient for antiviral potency.[11] It is the high dissociation rate constants that render aminoadamantanes useless against S31N viruses like WSN leading to K_d (TEVC) in the millimolar range compared to the micromolar range for M2 WT binding.

In the S31N variants, TEVC (Table 4) shows very high exit rate constants, especially for **2** (0.9 s^{-1}) and **5** (0.14 s^{-1}), consistent with the unmeasurably high K_d in ITC (Table 1, lower) and EC_{50} in CPE (Table 2, WSN). Interestingly, in these two cases, **2** and **5** have low % block of inward currents at 2, 5, and 10 min in Udorn M2 S31N (Table 4), and somewhat similar k_{on} rates to **1** and **3**, albeit lower compared to M2 WT, (Table 3), demonstrating that mutations can have complex, ligand-dependent effects on entry and exit rates.

M2TM WT complexes were simulated using an experimental structure of M2TM WT (PDB ID 2KQT[4,8]) determined at pH 7.5 in the presence of **1** (see ref 11 for details). No significant differences in measures were detected between trajectories with production times of 4 and 80 ns (Tables S2 and S3). To ensure that the measures were meaningful, the equilibration of the membranes was tested. To verify this, the average area per lipid headgroup was measured in the simulation of the different lipids and compared with experimental results.[23] The calculated values approached the experimental ones of pure lipid bilayers (see Figure S4 and Table S5). The center of mass between the four V27 residues and the adamantane cage of the ligand stabilized as explained in Figure 1 varies between 4.1 and 4.5 Å on average (Tables S2 and S3). Hydrogen bond interactions for **2**-*R* and **2**-S and geometric measures, which reflect van der Waals contacts, were found to be similar for the two enantiomers, suggesting equal binding interactions as previously discussed (Figure S3).[17] In diethyl and di-*n*-propyl derivatives (**4** and **5**), the alkyl groups seem to better fill the space between the ligand and the pore walls; but in these cases, restricted motion and the resulting entropy cost of binding may be significant and decrease the

DOI: 10.1021/acsmedchemlett.7b00458
ACS Med. Chem. Lett. 2018, 9, 198−203

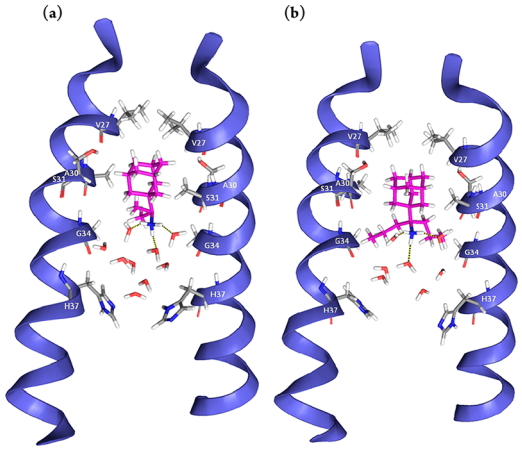

Figure 1. Representative snapshots from the simulation of ligands **3** (a) and **5** (b) bound to M2TM WT. Nine and seven water molecules are shown between the ligand and H37 residues for **3** and **5**, respectively. Three hydrogen bonds between the ammonium group of the ligand and three water molecules are shown. Hydrogen bonding with water molecules and van der Waals interactions of the adamantane core with V27 and A30 side chains stabilize the ligand inside the pore with its ammonium group oriented towards the C-terminus of the channel.

binding affinities compared to **3** (Tables 1−3 and S1). Configurations from the simulations of ligands **3** and **5** are depicted in Figure 1. In all cases, in the region located above the adamantane core (i.e., toward the N-terminus) no water molecules were found, which is consistent with the proton blocking effect of the aminoadamantane derivatives.[2,11,22,24]

The MD simulations of the complex of **3** or **5** with M2TM S31N showed that the ligand cannot bind tightly to M2TM S31N because significant favorable van der Waals interactions are missing (Figure 2). The S31N mutation of M2TM results in a shift of the hydrophobic adamantyl ring toward the C-terminus, due to the enhanced repulsive forces of the asparagine amide side chains to the adamantyl ring and attraction to water molecules. As a consequence, the stabilizing hydrophobic interactions of the

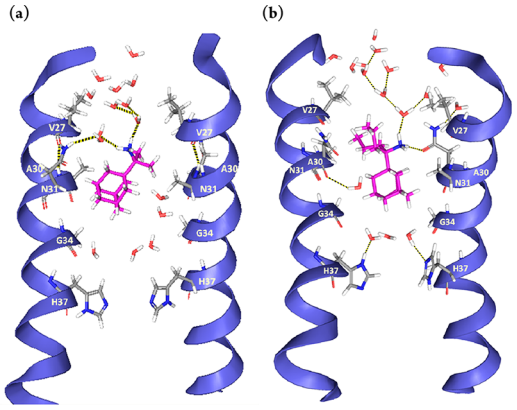

Figure 2. Representative snapshots from the simulations of ligand **3** (a) and **5** (b) bound to M2TM S31N. Five and three water molecules are shown between ligand **3** and **5**, respectively, and the H37 residues and ten and twelve water molecules, respectively, between N31 and the mouth of the pore. The ammonium group of the ligand is oriented towards the N-terminus, where it forms hydrogen bonds with water molecules or the carbonyl group of the N31 amide side chain. The loss of the V27 pocket for the adamantyl cage would be expected to lead to weak binding of aminoadamantane ligands.

V27 isopropyl groups with the adamantyl ring that are present in the M2TM WT are lost in M2TM S31N.[11] The bulky Val27 and N31 side chains are oriented toward the N-terminus the latter forming hydrogen bonding interactions with water molecules; the ammonium group of the ligands are also turned toward the N-terminus, allowing significant hydrogen bonding interactions with the polar N31 side chains and the nearby water molecules.[11] The hydrogen bonding interactions with N31 are consistent with our magic angle spinning (MAS) experimental data for spiro[pyrrolidine-2,2′-adamantane]−M2TM S31N complex. With the adamantane compound present, there was a chemical shift perturbation for N31 and G34 compared to the *apo* M2TM S31N.[11] In the M2TM WT, the adamantyl ring is well accommodated by the V27 and A30 side chains, and sizable adducts such as ligands **4** and **5** additionally fill the region between A30 and G34 (Figure 1); but in M2TM S31N, the adamantyl ring is between A30 and G34 (Figure 2), due to the lack of a favorable hydrophobic pocket. We have also found[11] an absence of chemical shift perturbations for V27 in M2TM S31N in presence of a bulky ligand, in comparison with the *apo* M2TM S31N, contrasting with the significant chemical shift changes at V27, S31, and G34 relative to the *apo* state reported when rimantadine is bound to M2TM WT.[17,22]

Compound **5** has sizeable adducts in addition to the adamantyl ring that can fill the region between A30 and G34, and the interactions needed for binding are slightly improved, resulting in weak binding to M2TM S31N according to ITC compared to no binding for **1**−**3** (Table 1). This can be observed from the snapshot for the complex of **5** with M2TM S31N in Figure 2b. The results showed no binding of **1** and similar in size analogues to M2 S31N and M2TM S31N, and only possible weak binding for sizable adducts in the region between A30 and G34, which is reflected by the high k_{off} values. The last point is in agreement with the results from MAS and OS ssNMR spectra.[11]

In summary, in this work, we compared the potency between the rimantadine analogues against M2 using four different M2 mimicry methods, i.e., ITC, MD simulations, EP, and antiviral assays. We investigated the binding kinetics of rimantadine analogues with M2 WT and M2 S31N and how they influenced the outcome of potency. We provided a kinetic perspective to explain rimantadine variant binding, proton transport blockage, and antiviral potency against influenza M2 WT and M2 S31N. According to this study, aminoadamantane variants bearing a polar head should exhibit a kinetic profile of small k_{off} rates (i.e., long residence time inside the M2 S31N protein channel pore) resulting in $K_d = k_{off}/k_{on}$ values at the low micromolar region, for them to exhibit inhibitory potency against M2 S31N protein.[25]

■ ASSOCIATED CONTENT

Supporting Information

The Supporting Information is available free of charge on the ACS Publications website at DOI: 10.1021/acsmedchemlett.7b00458.

Experimental and MD simulations additional material (PDF)

■ AUTHOR INFORMATION

Corresponding Author

*Tel: (+301) 210-7274834. Fax: (+301) 210 727 4747. E-mail: ankol@pharm.uoa.gr.

ORCID

Jun Wang: 0000-0002-4845-4621

DOI: 10.1021/acsmedchemlett.7b00458
ACS Med. Chem. Lett. 2018, 9, 198−203

Antonios Kolocouris: 0000-0001-6110-1903

Present Address

A.D.: Pharmaceutical and Medicinal Chemistry, Institute of Pharmacy and Food Chemistry, Julius-Maximilians-Universität Würzburg, Am Hubland, 97074 Würzburg, Germany.

Author Contributions

A.K. designed this research project. A.D. and C.T. contributed equally. A.D. and C.T. did ligand synthesis. C.T., A.D., Ath.K., and D.K. did the MD simulations. C.M. in J.W. group did the EP experiments against the Udorn M2 and WSN M2 N31S and the plague reduction assay against Udorn virus. K.M. in D.B. group did the EP experiments against the Udorn M2 and kinetic measurements. K.F. and J.H. in G.G. group did the ITC measurements. A.H. in the M.S. group performed CPE inhibitory assays with WSN M2 N31S and HK virus and plague reduction assay against Udorn virus as well as the cytotoxicity determinations. A.K. wrote the manuscript, and J.W., M.S., A.H., A.D., and D.B. revised it. This research includes part of the Master thesis work of A.D. and part of the Ph.D. work of C.T.

Notes

The authors declare no competing financial interest.

■ ACKNOWLEDGMENTS

We are grateful to Chiesi Hellas for supporting this research and the Ph.D. work of C.T.; J.W. thanks the support from NIH AI119187 and PhRMA Foundation 2015 Research Starter Grant in Pharmacology and Toxicology; A.H. and M.S. thank Andreas Sauerbrei for continuous kind support; A.K. and M.S. thank Professor Adolfo Garcia-Sastre group and the CEIRS program (NIAD Centers of Excellence for Influenza Research and Surveillance) for providing the Udorn virus.

■ REFERENCES

(1) Ferruz, N.; De Fabritiis, G. Binding Kinetics in Drug Discovery. *Mol. Inf.* **2016**, *35*, 216−226.

(2) Wang, C.; Takeuchi, K.; Pinto, L. H.; Lamb, R. A. Ion Channel Activity of Influenza A Virus M2 Protein: Characterization of the Amantadine Block. *J. Virol.* **1993**, *67*, 5585−5594.

(3) Hayden, F. G. Clinical Applications of Antiviral Agents for Chemophrophylaxis and Therapy of Respiratory Viral Infections. *Antiviral Res.* **1985**, *5*, 229−239.

(4) Hu, J.; Asbury, T.; Achuthan, S.; Li, C.; Bertram, R.; Quine, J. R.; Fu, R.; Cross, T. A. Backbone Structure of the Amantadine-Blocked Trans-Membrane Domain M2 Proton Channel from Influenza A Virus. *Biophys. J.* **2007**, *92*, 4335−4343.

(5) Schnell, J. R.; Chou, J. J. Structure and Mechanism of the M2 Proton Channel of Influenza A Virus. *Nature* **2008**, *451*, 591−595.

(6) Stouffer, A. L.; Acharya, R.; Salom, D.; Levine, A. S.; Di Costanzo, L.; Soto, C. S.; Tereshko, V.; Nanda, V.; Stayrook, S.; DeGrado, W. F. Structural Basis for the Function and Inhibition of an Influenza Virus Proton Channel. *Nature* **2008**, *451*, 596−599.

(7) Cady, S. D.; Mishanina, T. V.; Hong, M. Structure of Amantadine-Bound M2 Transmembrane Peptide of Influenza A in Lipid Bilayers from Magic-Angle-Spinning Solid-State NMR: The Role of Ser31 in Amantadine Binding. *J. Mol. Biol.* **2009**, *385*, 1127−1141.

(8) Cady, S. D.; Schmidt-Rohr, K.; Wang, J.; Soto, C. S.; DeGrado, W. F.; Hong, M. Structure of the Amantadine Binding Site of Influenza M2 Proton Channels in Lipid Bilayers. *Nature* **2010**, *463*, 689−692.

(9) Cady, S. D.; Wang, J.; Wu, Y.; Degrado, W. F.; Hong, M. Specific Binding of Adamantane Drugs and Direction of Their Polar Amines in the Pore of the Influenza M2 Transmembrane Domain in Lipid Bilayers and Dodecylphosphocholine Micelles Determined by NMR Spectroscopy. *J. Am. Chem. Soc.* **2011**, *133*, 4274−4284.

(10) CDC. High Levels of Adamantane Resistance among Influenza A (H3N2) Viruses and Interim Guidelines for Use of Antiviral Agents–United States, 2005−06 Influenza Season. *MMWR. Morb. Mortal. Wkly. Rep.* **2006**, *55*, 44−46.

(11) Tzitzoglaki, C.; Wright, A.; Freudenberger, K.; Hoffmann, A.; Tietjen, I.; Stylianakis, I.; Kolarov, F.; Fedida, D.; Schmidtke, M.; Gauglitz, G.; Cross, T. A.; Kolocouris, A. Binding and Proton Blockage by Amantadine Variants of the Influenza M2 $_{WT}$ and M2 $_{S31N}$ Explained. *J. Med. Chem.* **2017**, *60*, 1716−1733.

(12) Ioannidis, H.; Drakopoulos, A.; Tzitzoglaki, C.; Homeyer, N.; Kolarov, F.; Gkeka, P.; Freudenberger, K.; Liolios, C.; Gauglitz, G.; Cournia, Z.; Gohlke, H.; Kolocouris, A. Alchemical Free Energy Calculations and Isothermal Titration Calorimetry Measurements of Aminoadamantanes Bound to the Closed State of Influenza A/M2TM. *J. Chem. Inf. Model.* **2016**, *56*, 862−876.

(13) Kolocouris, A.; Tzitzoglaki, C.; Johnson, F. B.; Zell, R.; Wright, A. K.; Cross, T. A.; Tietjen, I.; Fedida, D.; Busath, D. D. Amino-adamantanes with Persistent in Vitro Efficacy against H1N1 (2009) Influenza A. *J. Med. Chem.* **2014**, *57*, 4629−4639.

(14) Kolocouris, N.; Foscolos, G. B.; Kolocouris, A.; Marakos, P.; Pouli, N.; Fytas, G.; Ikeda, S.; De Clercq, E. Synthesis and Antiviral Activity Evaluation of Some Aminoadamantane Derivatives. *J. Med. Chem.* **1994**, *37*, 2896−2902.

(15) Fan, Z.; Shu, S.; Ni, J.; Yao, Q.; Zhang, A. Ligand-Promoted Pd(II)-Catalyzed Functionalization of Unactivated C (sp3)−H Bond: Regio- and Stereoselective Synthesis of Arylated Rimantadine Derivatives. *ACS Catal.* **2016**, *6*, 769−774.

(16) Salom, D.; Hill, B. R.; Lear, J. D.; DeGrado, W. F. pH-Dependent Tetramerization and Amantadine Binding of the Transmembrane Helix of M2 from the Influenza A Virus. *Biochemistry* **2000**, *39*, 14160−14170.

(17) Drakopoulos, A.; Tzitzoglaki, C.; Ma, C.; Freudenberger, K.; Hoffmann, A.; Hu, Y.; Gauglitz, G.; Schmidtke, M.; Wang, J.; Kolocouris, A. Affinity of Rimantadine Enantiomers against Influenza A/M2 Protein Revisited. *ACS Med. Chem. Lett.* **2017**, *8*, 145−150.

(18) Rosenberg, M. R.; Casarotto, M. G. Coexistence of Two Adamantane Binding Sites in the Influenza A M2 Ion Channel. *Proc. Natl. Acad. Sci. U. S. A.* **2010**, *107*, 13866−13871.

(19) Schmidtke, M.; Schnittler, U.; Jahn, B.; Dahse, H.-M.; Stelzner, A. A Rapid Assay for Evaluation of Antiviral Activity against Coxsackie Virus B3, Influenza Virus A, and Herpes Simplex Virus Type 1. *J. Virol. Methods* **2001**, *95*, 133−143.

(20) Barniol-Xicota, M.; Gazzarrini, S.; Torres, E.; Hu, Y.; Wang, J.; Naesens, L.; Moroni, A.; Vázquez, S. Slow but Steady Wins the Race: Dissimilarities among New Dual Inhibitors of the Wild-Type and the V27A Mutant M2 Channels of Influenza A Virus. *J. Med. Chem.* **2017**, *60*, 3727−3738.

(21) Wang, J. J.; Wu, Y.; Ma, C.; Fiorin, G.; Pinto, L. H.; Lamb, R. A.; Klein, M. L.; Degrado, W. F. Structure and Inhibition of the Drug-Resistant S31N Mutant of the M2 Ion Channel of Influenza A Virus. *Proc. Natl. Acad. Sci. U. S. A.* **2013**, *110*, 1315−1320.

(22) Wright, A. K.; Batsomboon, P.; Dai, J.; Hung, I.; Zhou, H. X.; Dudley, G. B.; Cross, T. A. Differential Binding of Rimantadine Enantiomers to Influenza A M2 Proton Channel. *J. Am. Chem. Soc.* **2016**, *138*, 1506−1509.

(23) Mori, T.; Ogushi, F.; Sugita, Y. Analysis of Lipid Surface Area in Protein-Membrane Systems Combining Voronoi Tessellation and Monte Carlo Integration Methods. *J. Comput. Chem.* **2012**, *33*, 286−293.

(24) Andreas, L. B.; Eddy, M. T.; Pielak, R. M.; Chou, J.; Griffin, R. G. Magic Angle Spinning NMR Investigation of Influenza A M2 $_{18-60}$: Support for an Allosteric Mechanism of Inhibition. *J. Am. Chem. Soc.* **2010**, *132*, 10958−10960.

(25) Wang, Y.; Hu, Y.; Xu, S.; Zhang, Y.; Musharrafieh, R.; Hau, R.-K.; Ma, C.; Wang, J. In Vitro Pharmacokinetic Optimizations of AM2-S31N Channel Blockers Led to the Discovery of Slow-Binding Inhibitors with Potent Antiviral Activity against Drug-Resistant Influenza A Viruses. *J. Med. Chem.* **2018**, DOI: 10.1021/acs.jmedchem.7b01536.

DOI: 10.1021/acsmedchemlett.7b00458
ACS Med. Chem. Lett. 2018, 9, 198−203